Penerbit Akademia Baru

Journal of Research in
Nanoscience and Nanotechnology

Journal homepage:
http://akademiabaru.com/submit/index.php/jrnn/index
ISSN: 2773-6180

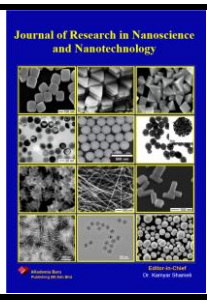

Formulation of Titanium Dioxide Nanoparticles Using Sol-gel Technique

Clera Peter John, Roshafima Rasit Ali*, Kamyar Shameli, Zatil Izzah Tarmizi, Mohd Shahrul Nizam Salleh and Justin Chan Zhe

Malaysia Japan International Institute of Technology, Universiti Teknologi Malaysia, Jalan Sultan Yahya Petra, 54100 Kuala Lumpur, Malaysia

* Correspondence: roshafima@utm.my; Tel.: +6016-7775724
https://doi.org/10.37934/jrnn.4.1.3548

ABSTRACT

Bio-based polymer has been extensively used as a plastic alternative for its ability of biodegradability. Currently, there is considerable interest in the self-cleaning and antimicrobial property of TiO_2 for applications in the food industry. In this research, TiO_2 nanoparticles (TiO_2 NPs) were formulated using the sol-gel method. The synthesis of TiO_2 NPs was carried out in varying pH condition which are in 1.5, 7 and 11. The optimize synthesized TiO_2 NPs powder was dispersed with bio-based polymer which is PLA to prepare self-cleaning bio-based polymer. 5 mL Titanium isopropoxide (TTIP) as a precursor, 15 mL of isopropanol act as a solvent, either ammonium hydroxide or hydrochloric acid with 250 mL of distilled water and 2% of honey as stabilizing and reducing agent were used to synthesized TiO_2 NPs. Then the suitable TiO_2 NPs were used to fabricate self-cleaning bio-based polymer. Characterization of the synthesized nanoparticles (NPs) with different pH condition and calcined temperature were investigated using Powder X-ray Diffraction (XRD) and Fourier Transform Infrared Spectroscopy (FTIR) was used to identify the presence of honey in TiO_2 NPs powder samples. From the XRD results, it proved that honey has been successfully reduced the crystallite size of the TiO_2 NPs and the optimal synthesized TiO_2 NPs was from an acidic condition with the calcined temperature of 400˚C. The size of obtaining TiO_2 NPs is calculated using Scherrer formula. The crystallite size of the fine pure anatase phase is 11.84 nm. Thus, the purpose of this research was achieved with the hydrophobic property, the bio-composite with the highest, the smaller TiO_2 NPs content in PLA will also exhibit self-cleaning ability which makes it suitable for the usage of hydrophobic food packaging material.

Keywords: Titanium dioxide nanoparticles, self-cleaning, bio-based plastics, sol-gel technique, crystallite size

Received: 23 August 2021 **Revised: 21 September 2021** **Accepted: 26 September 2021** **Published: 17 October 2021**

1. Introduction

The biodegradable packaging market is expected to be valued at USD 935.9 billion in 2021 and will reach a value of USD 126.8 billion by 2026, at a CAGR of 5.3% over the forecast period (2021 to 2026) [1]. Moreover, biodegradable packaging solutions have a low environmental impact, increasing attention to recyclability and sustainability. The government's emphasis on effective package management, plastic restrictions, and growing consumer consciousness are expanding their applicability to packaging. Packaging waste, particularly waste from non-biodegradable polymers, is a major component of municipal solid waste and is of growing concern for the environment [2]. Discarded packaging presents a huge challenge to waste management as it appears to be a very visible source of waste. The petroleum-based polymer which is known as polyethylene (PE) is the most extensively utilized in packaging applications [3,4]. Other petroleum-based polymers or PE are exceedingly difficult to biodegrade after disposal on land or offshore, resulting in different contamination level.

Although bio-based polymers are environmentally friendly and most attractive packaging materials, there industrial applications are limited because of some factors such as their oxygen/water vapor barriers, thermal resistance and other mechanical properties related with costs [5]. Due to these limitations, synthetic polymers are the most widely used materials for packaging. To address these limitations and encourage the industrial applications of bio-based polymers for packaging materials, there is the need for further research to effectively enhance their shelf-life, quality, nutritional values and microbial resistance [6]. Additionally, the barrier properties need to be enhanced. Several methods of enhancing the properties and performance of antimicrobial packaging materials such as polymeric blending, chemical and physical modifications, nanocomposites, have demonstrated promising potential for various applications [5,6].

Both functional and technical limitations have also been barriers to the development and applications of antimicrobial packaging materials in the food industry. Some of these limitations are include vapor and air barriers, the low process ability of bio-based plastics, the stability of antimicrobial agents under processing conditions, toxicity as well as the changes in mechanical properties of the packaging materials. However, to maintain food freshness and quality, it is necessary to choose the correct materials and packaging technologies. On the other hand, the bio-based film's biggest flaws are high permeability to water vapor transfer and the ease of spoilage by bacteria and fungi [5,6,7,8]. The circular economy has to be reached in every corner of life, and, at the same time, we must be able to combat bacterial resistance to antibiotics.

In a general scenario, water droplets generate a thin layer on the surface of a hydrophilic surface during the self-cleaning process, and this uniform spreading allows for faster drying and greater surface visibility. To put it another way, it keeps the surfaces from fogging up. On the other hand, on hydrophobic surfaces, the droplets roll over the surface, carrying the dirt away [9]. Titanium dioxide is one of the most often utilized materials for photocatalytic with self-cleaning surfaces. This oxide is a chemically inert and non-toxic semiconductor with long availability, durability, and relatively low cost [9,10]. Metal oxide nanoparticles synthesis processes may be classified into two categories which are through physical technique such as sputtering, ball milling, electron beam evaporation, electro-spraying, and laser ablation or by chemical technique include the chemical vapor deposition, polyol method, sol – gel process, hydrothermal method, micro-emulsion technique, and co-precipitation method [11].

The physical method provides a top-to-bottom approach. In other words, it starts with the bulk counterpart of the material, which is systematically depleted for the formation of synthetic tiny nanoparticles, while the chemical technique is mostly bottom-up [12]. A group of atoms or molecules

that together generate a dispersion of nanoparticles of various sizes. Chemical approaches have the benefit of allowing the production of particles with precise dimension, size, structure, and composition which might be beneficial in a variety of applications like sensing, electrical devices, and catalysis [11,13]. Furthermore, synthesis using some chemical techniques, notably the sol–gel technique, needs lower processing less energy and temperatures, making this approach more cost effective than physical approaches [14]. The characteristics of nanoparticles (NPs) are directly influenced by their size and shape. A framework that enables for more control over the size and shape of the NPs is ideally suited for a wide range of application. Several studies have indicated that the sol–gel technique is one of the most promising approaches for manipulating the size and shape of nanoparticles [15].

This research focused on the type of phase and size of the crystallite, which appears to be the most promising domain from a sustainability stance. TiO_2 nanoparticles (TiO_2 NPs) with bio-based plastic is an outstanding combination to formulate a unique 'lotus-effect' characteristics to improve its application. 'Lotus-effect' is recognized as the ability to self-clean due to the hydrophobic properties [16]. This implies that the surfaces will repel contaminants such as organic liquids, solid particles, and biological contaminants with a hint of water drop [17]. As well as that, bio-based polymers are outstanding candidates to be modified or combined with an antimicrobial substance to obtain antimicrobial systems with application in several fields and in good alignment with the circular economy. Thus, in this research, a bio-based plastic with self-cleaning properties has been fabricated by synthesized TiO_2 NPs powder which having a superhydrophobic and antimicrobial characteristics.

2. Materials and Methods

All of the chemicals used were analytical grade and were acquired from Sigma-Aldrich. They were used as obtained without any additional purification. The chemicals used in the research are Ttitanium tetraisopropoxide (TTIP), Dichloromethane (DCM), Isopropanol, commonly known as Isopropyl alcohol, Hydrochloric acid (HCl), Ammonia (NH_3) and Hexadecyltrimethylammonium bromide (CTAB). Apart from this, materials such as polylactic acid (PLA) was also purchased from Sigma-Aldrich while honey (capilona) was obtained from the convenience store (99-Speedmart Sdn. Bhd, Malaysia). Dionized water was utilized in the preparation of all aqueous solutions. The list of chemicals applied in this research, along with their characteristics, are illustrated in Table 1.

Table 1. List of the chemicals that have been acquired, along with their properties.

Chemicals	Purchase	Properties				
		Chemical Formula	**Molecular Weight** ($gmol^{-1}$)	**Boiling Point** (°C)	**Melting Point** (°C)	**Appearance**
TTIP	Sigma-Aldrich (M) Sdn Bhd, Malaysia	$Ti[OCH(CH_3)_2]_4$	284.22	232	17	Pale-yellow liquid
DCM	Sigma-Aldrich (M) Sdn Bhd, Malaysia	CH_2Cl_2	84.93	39.75	-97	Colourless liquid

Isopropanol	Sigma-Aldrich (M) Sdn Bhd, Malaysia	C_3H_8O	60.09	82.6	−89	Colourless liquid
HCl	Sigma-Aldrich (M) Sdn Bhd, Malaysia	HCl	36.46	57	-35	Colourless liquid
NH_3	Sigma-Aldrich (M) Sdn Bhd, Malaysia	NH_3	17.03	60	-78	Colourless liquid
CTAB	Sigma-Aldrich (M) Sdn Bhd, Malaysia	$C_{19}H_{42}BrN$	364.448	235	218 to 247	Crystalline white powder
PLA	Sigma-Aldrich (M) Sdn Bhd, Malaysia	$(C_3H_4O_2)n$	60,000	-	175 to 220	Amorphous white resins
Honey	99-Speedmart Sdn. Bhd, Malaysia	$C_6H_{12}O_6$	180.16	85	40 to 50	Dark golden viscous liquid

2.1. Synthesis of TiO_2 NPs

A 250 mL solution of dionized water was measured and poured into four different beakers. Then, the pH condition for each of the solution was adjusted until it reaches 1.5 using 36% weight of HCl as the hydrolysis catalyst. Then, honey was measured 2% of distilled water volume and it was mixed well together in each of the beaker with the pH 1.5. Meanwhile, in four sets of 500 mL beaker, 15 mL of isopropanol was poured, respectively. About 5.0 mL of (TTIP) was added slowly using micro-pipette into each of the beaker where consequently the colourless solution turned into a yellowish-white solution.

The mixtures were allowed to heat in a hot plate until it reaches 70˚C while stirred vigorously at 510 rpm and yellowish gel were formed. The prepared 250 mL solutions were poured gently into the mixtures, respectively. The mixing was occurred meanwhile it have been stirred vigorously at 510 rpm where the yellowish gel instantly turned into a cloudy solution. The mixing was continued for 16 hours with the vigorous stirring at 510 rpm and the temperature was maintained at 70˚C. At this point, peptization process took place. The volume of the solutions was reduced to 50 mL from each of the beaker after the peptization process, and a suspension were started to form at this stage, Subsequently, the resulting suspension formed was dark orange with high viscosity, depending on the preparation conditions.

Later, the dark orange precipitates were then washed three time with ethanol using centrifuge. Then, it was allowed to be dried in vacuum oven for 3 hours at 100˚C in order to remove moisture content. A brownish-yellow powders are obtained. Finally, the obtained four respective powders

were heated for 2 hours at the temperatures of 200˚C, 400˚C, 600˚C and 800˚C to eliminate the remaining impurities. Above procedure were repeated by adjusting the pH value to 7 and 11 using ammonia solution. Then, the procedure was repeated without adding honey into the solution with pH value of 7. The obtained samples of TiO_2 NPs were characterized with X-ray diffraction (XRD) using XRD-Empyrean (PAN anaytical, United Kingdom). Analysis pattern of XRD was adjusted at 2θ angle from 5˚C to 90˚C. The diameters of the crystallite were calculated using Scherrer's formula with the XRD analysis, as written in equation 1.

$$d = \frac{k\lambda}{\beta\cos\theta} \quad (1)$$

Where,
d = Diameters of the crystallites
β = Full-width at half-maximum of the diffraction peaks
k = Shape factor which is 0.9 for spherical particles
λ = X-ray wavelength (nm)
θ = Diffraction angle

Besides, Fourier Transform Infrared (FTIR) Spectrometer Frontier version 10.5.2 were used to characterize the chemical structure and identify the presences of functional group of honey in the obtained TiO_2 NPs.

2.2. Fabrication of self-cleaning bio-based plastic using casting method.

During bio-based plastic preparation four different weight ratio of TiO_2 NPs were selected to be dispersed into PLA which are 0.1, 0.5, 1.0 and 5.0 wt%. Approximately, 5.0 g of PLA was weighed and added into 25 mL of DCM. This mixture is mixed vigorously at 900 rpm until the PLA was completely dissolve. 0.1 wt% of selected TiO_2 NPs powder was mixed with CTAB at the ratio of 1:1 together with 25 mL of DCM. Then this solution is allowed to undergo dispersion in ultrasonics machine for about 20 minutes. The mixture later added into 25 mL of dissolved PLA with a vigorous stir at 700 rpm for 20 minutes. The well mixed solution then poured into a petri dish, and it was left inside the fume hood to dry for 2 days. The procedure was repeated by replacing 0.1 to 0.5, 1.0 and 5.0 wt% of TiO_2 NPs powder.

3. Results and Discussion

3.1. Synthesis of TiO_2 NPs powder

The synthesis of TiO_2 NPs powder was successfully formulated using sol-gel method. The sol-gel method is a wet-chemical technique used mostly in ceramic engineering and materials science. It is described as the transformation of a precursor solution into an inorganic solid by water-induced polymerization processes. Hydrolysis produces a sol, which is essentially a liquid dispersion of colloidal particles, and condensation produces a gel. The sol-gel technique is extremely promising for the synthesis and synthesis of inorganic and organic-inorganic hybrid nanomaterials since it occurs in a relatively low temperature (below 100°C) and the molecular level composition uniformity.

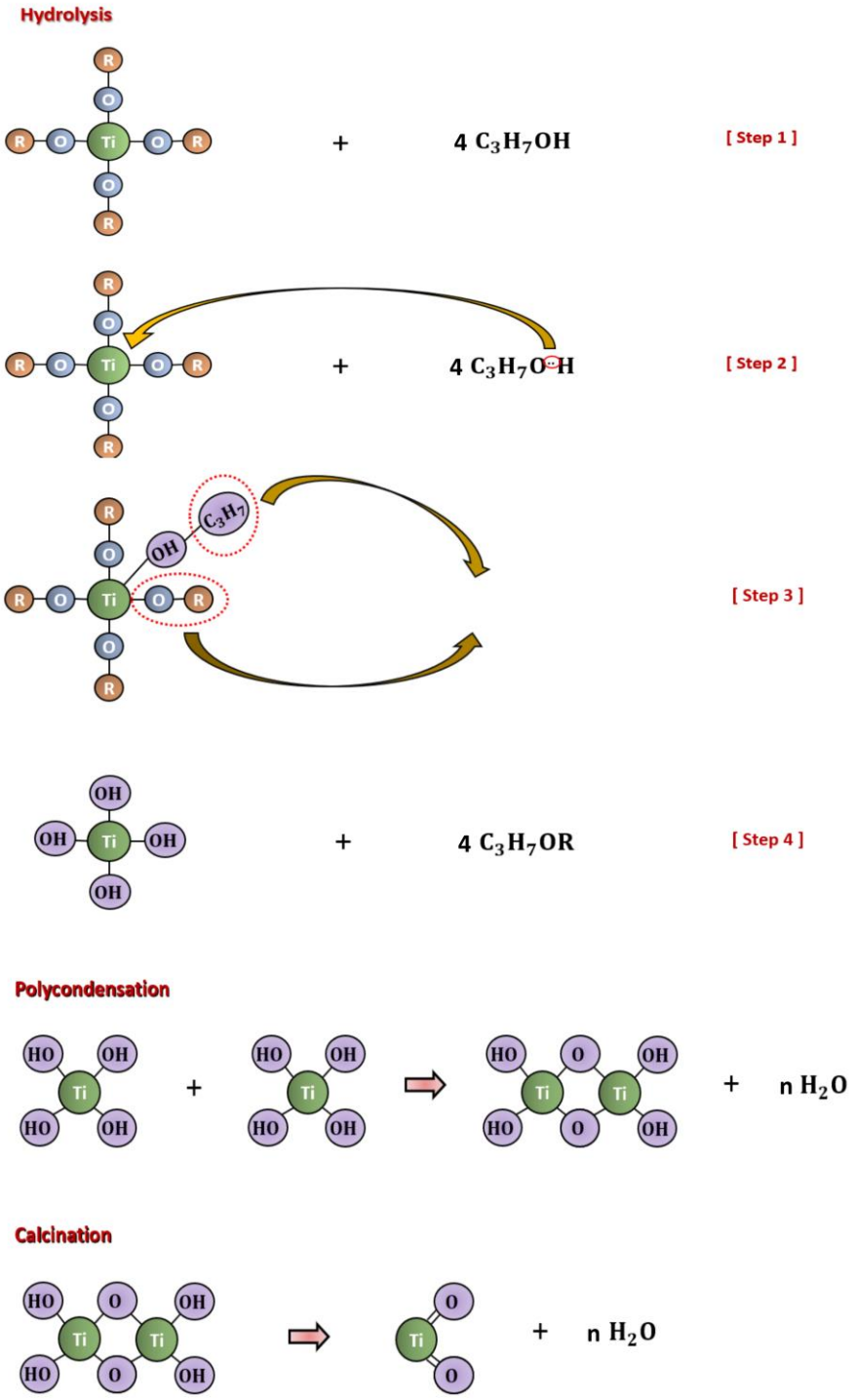

Figure 1. Mechanism of TiO_2 NPs using sol-gel method.

The sol-gel technique generates fine, uniformly sized spherical powders and this has been widely used to synthesized TiO_2 materials. Metal oxides and metal chlorides are prominent precursors. An M-O-R bond, in which O is oxygen, M is the metal, and R is an alkyl group, forms up a metal alkoxide. Because of the polarization that occurs in the M-O bond, it is susceptible to nucleophilic attacks. The alcoholic $OH^{\delta-}$ group nucleophilically adds to the titanium cations as shown in Figure 1 in step 2. However, step 3 involves a non-transition state transfer between the negatively charged OR group and the positively charged C_3H_8 group. Besides, separation of the positively charged OR ligand takes

place in step 4. The OR group is replaced by an OH group as a result of these reactions, resulting in titanium hydroxides that are subjected to condensation. Condensation is the process by which metal hydroxide groups interact to form a hydrated metal-oxide network, which subsequently produces small nuclei. To synthesize both polymeric and particulate titanium sols, the chemistry, hydrolysis, and polycondensation processes are highly convenient. Polycondensation is the process through which monomers become oligomers and then polymers. Complex random branching may develop if the number of alkoxide groups is larger than 2, eventually leading to fractal formations. Metal alkoxides employed in the sol-gel method are typically extremely reactive, necessitating the use of modifiers or the inclusion of chelating ligands such as carboxylic acids, β-diketones, or other complex ligands to control the reactivity and obtain sols and gels with desirable characteristics. These modifiers react with alkoxides to produce novel molecular precursors that may be utilized in sol-gel processing to improve hydrolysis-condensation control processes. This novel precursor limit reactivity and functionality, inhibit condensation, and result in the formation of smaller species. The quantity of M-O-R bonds accessible for hydrolysis is reduced by modifiers and decreasing hydrolytic susceptibility. Because β-diketones are employed as surface capping reagents and polymerization locks, they reduce nuclearity, resulting in small particles. Hydrochloric acid and other carboxylate ligands are primarily used as bridge chelating ligands. The sol-gel approach has a number of strengths, which includes the usage of low temperatures during the preparation, simple and efficient control of size of particles, shape, and characteristics, improved homogeneity from raw resources, improved purity from precursor materials, the ability to design the material structure and properties through proper precursor selection. The fundamental objective of this research was to enhance the homogeneity and crystallinity of TiO_2 NPs as a function of reflux time. The powder crystallinity was investigated using the findings of XRD analysis and the presence of honey was identified using FTIR analysis.

3.2. X-Ray Powder Diffraction (XRD) Analysis

Diffraction patterns and crystallite size of synthetized TiO_2 NPs powder were studied using XRD. Figure 2 below shows the XRD patterns for the synthesized TiO_2 NPs after calcined with varies in calcination temperature.

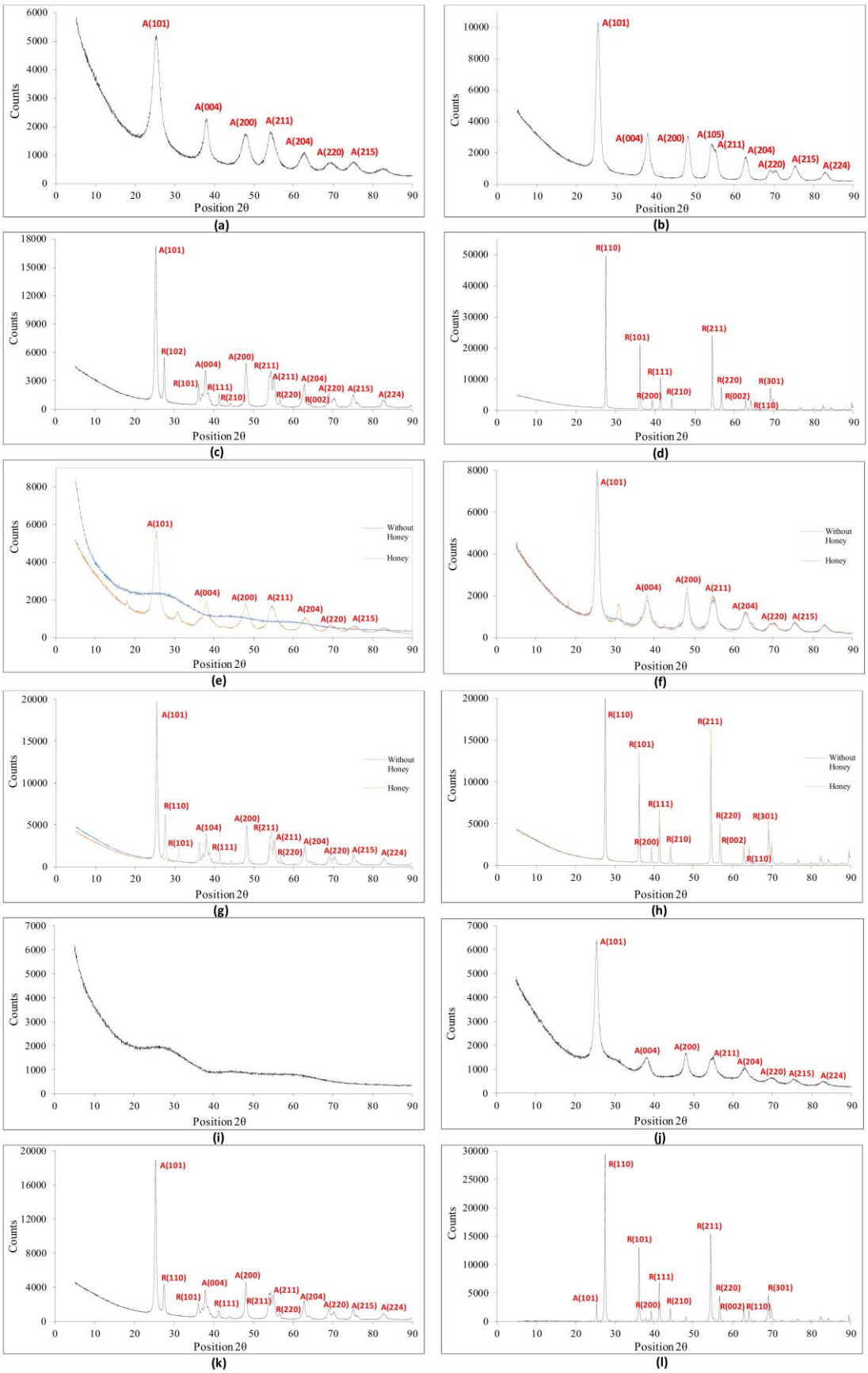

Figure 2. XRD patterns for varies pH conditions annealed at different temperature: (a) Pure synthesized TiO_2 NPs at 200°C in acidic medium with honey, (b) Pure synthesized TiO_2 NPs at 400°C in acidic medium with honey, (c) Pure synthesized TiO_2 NPs at 600°C in acidic medium with honey,

(d) Pure synthesized TiO_2 NPs at 800°C in acidic medium with honey, (e) Pure synthesized TiO_2 NPs at 200°C in neutral medium with and without honey, (f) Pure synthesized TiO_2 NPs at 400°C in neutral medium with and without honey, (g) Pure synthesized TiO_2 NPs at 600°C in neutral medium with and without honey, (h) Pure synthesized TiO_2 NPs at 800°C in neutral medium with and without honey (A: Anatase, R: Rutile), (i) Pure synthesized TiO_2 NPs at 200°C in alkali medium with honey, (j) Pure synthesized TiO_2 NPs at 400°C in alkali medium with honey, (k) Pure synthesized TiO_2 NPs at 600°C in alkali medium with honey, and (l) Pure synthesized TiO_2 NPs at 800°C in alkali medium with honey (A: Anatase and R: Rutile).

The crystal structure and phase composition of the synthesized powder samples were investigated using XRD. XRD of TiO_2 NPs synthesized at various calcined temperatures are shown in Figure 2, along with the associated indices of the various diffraction planes, which R and A denote rutile and anatase respectively. Structure of anatase and rutile were found in the NPs. In pH 1.5 and 7 condition, the anatase phase was visible in the particles synthesized at 200°C, while the anatase and rutile phases were visible in the particles when the powder calcined at 600°C, and the rutile phase was visible in the particles annealed at 600°C as shown in Figure 2(c). Crystallite development and enhanced crystalline character of the samples are shown by a rise in diffraction intensity as the calcination temperature increases. The hydroxyl radicals (OH–) were adsorbed effectively into the nanomaterials synthesized at greater temperatures and even with large grain sizes, results in an increase in the magnitude of the diffraction peaks with increasing temperature. When the temperature was increased over 400°C, the (1 1 0) plane became visible. At 600°C, the strongest peak was found in the (1 1 0) plane of the stable rutile tetragonal phase. It has been observed that the anatase phase of TiO_2 NPs has higher stability. The rutile structural content of the particles calcined until it reaches 400°C is believed to be 0% since there is no visible rutile phase as shown in Table 2. Similarly, there is no anatase phase in the XRD patterns for particles calcined at 800°C, and the rutile structure composition is considered to be 100%. The direct/indirect bandgap behaviour of these phases is to responsible for the difference in activity between anatase and rutile. Indeed, anatase has been demonstrated to behave as an indirect semiconductor, with selection criteria prohibiting electron desexcitation from the conduction band to the valence band. As a result, anatase has a longer electron-hole lifetime than rutile, which behaves as a direct semiconductor with a shorter carrier lifetime.

3.2.1. Effect of pH Condition and Calcination Temperature

As shown in Figure 2(b) and (f), after calcining TiO_2 NPs powder at 400°C for 2 hours at pH 1.5 and 7 a single-phase anatase structure was formed. It can be seen that in the condition pH 1.5 and 7 the crystal planes of (1 0 1), (0 0 4), (2 0 0), (2 1 1), (2 0 4), (2 2 0), and (2 1 5) correlate to the diffraction peak at 25.4°, 38.1°, 48°, 54.2°, 63.2°, 69.5°, 75.5°, and 82.8° respectively, showing the development of anatase phase of TiO_2 NPs. The peaks of the plot correlate to the conclusions of the study report, which has been attached in the appendix. The presence of TiO_2 NPs was confirmed when the position of the peaks was matched to published values. Meanwhile in pH 11, the formation of TiO_2 NPs does not appear until the calcination temperature increases above 200°C as shown in Figure 2(i), whereas in acidic and neural conditions the peaks started to be appeared at 200°C. The partial charge model can be used to describe this mechanism. According to this concept, titanium cation hydrolysis occurs in conditions of high acidity. A stable species of $[Ti(OH)(OH_2)_5]^{3+}$ will form in this condition, however due to the positive charge of the hydroxo group, this species will not condense. Deprotonation occurs when the acidity is not low enough to stabilize these precursors, resulting in the formation of new

species of $[Ti(OH)_2(OH_2)_5]^{2+}$. Because of spontaneous intramolecular oxolation to $[TiO(OH_2)_5]^{2+}$, these species do not condense. When solution activity is strong enough to allow further deprotonation to $[TiO(OH)(OH_2)_4]^{+}$, which can then undergo intermolecular deoxolation to $[TiO(OH)_3(OH_2)_3]^{+}$ depending on pH, condensation to anatase and rutile starts. Deoxolation does not occur at lower pH levels, and oxolation causes cation linear growth in the equatorial plane. Because of the oxolation between the resultant linear chains, rutile is formed. Meanwhile, when deoxolation happens at higher pH levels, condensation can proceed in an apical direction, resulting in the skewed chain of anatase structure. As a result of this research, it is believed that pH values influence the determination of the resultant crystal structure. Higher acidity increases the production of anatase, whereas lower acidity stimulates the formation of rutile. The prominent diffraction peaks corresponding to the (1 0 1) plane are depicted in Figure 2. The calculated crystallite sizes were summarized in Table 2. From Table 2, it can be observed that the particle size in all cases is less than 34.49 nm, and the smallest crystallite was synthesized using this method is 8.93 in an acidic condition and calcined at 200 °C. The obtained XRD results are in line studies on the synthesis of catalyst nanoparticles using the sol-gel and solvothermal techniques. The occurrence of smaller crystallite size was ascribed to the wider diffraction peaks matching to the solvothermal derived sample. Pure anatase phase was shown to be more favourable when a acid condition was used. In most instances, greater calcination temperatures resulted in rutile formation, which is more stable structure than anatase and brookite. However, the obtained TiO_2 NPs powder at 200°C in acidic condition will not be chosen even though the size of TiO_2 NPs has the smallest size. This is because, according to the obtained appearance of synthesized NPs powder, it indicates that the powder still contained with the impurities since the powder is not in white colour due to the incomplete calcined process. Moreover, the particle size grew larger as the pH value increased. The powders were composed of small, soft agglomerates as summarized in Table 2. Particles get larger and clump together at higher pH levels. Several investigations have found that the pH affects the diversity of TiO_2 NPs surface charge. Because of the absorption of H^+ or OH^- in aqueous solution, TiO_2 in sols has an electrical charge. Chemisorption's of TiO_2 can be used to estimate its surface charges.

Table 2. Synthesized TiO_2 NPs sizes and phases under various temperature and pH conditions.

pH	**Temperature** (°C)	**200**	**400**	**600**	**800**
		Phase (nm)			
1.5	Anatase	8.93	11.84	14.15	-
	Rutile	-	-	19.00	34.49
7 (With Honey)	Anatase	14.02	15.31	15.63	-
	Rutile	-	-	21.04	31.66
7 (Without Honey)	Anatase	-	17.77	21.88	-
	Rutile	-	-	23.04	31.66
11	Anatase	-	24.54	29.62	-
	Rutile	-	12.34	20.6	25.16

In Acidic Condition (H^+);

$$TiO_2 + nH^+ \leftrightarrow TiO_2H_n^{n+} \text{ for pH 1.5} \quad (2)$$

In Alkaline Condition (OH^-);

$$TiO_2 + nOH^- \leftrightarrow TiO_2(OH)_n^{n-} \text{ for pH 11} \quad (3)$$

The significant repulsive charge among particles in acidic and alkaline environments lowers the probability of coalescence, allowing for the formation of more stable sols as shown in eq (2) and eq (3) [18]. The isoelectricity of TiO_2 NPs changes across pH ranges. According to this research, because the sample synthesized at pH 1.5 is beyond the range of isoelectric point when the calcined temperature increases, it forms less aggregates and larger TiO_2 particles. Lower pH promotes anatase TiO_2 NPs formation in the presence of rutile TiO_2 NPs impurities. An enlarged anatase (1 0 1) peak of TiO_2 NPs at various pH levels is shown in Figure 3. As the concentration of H^+ increased, the diffraction peaks moved slightly to the higher angle side. This peak shift might be due to the TiO_2 NPs developing various types of strain (tensile and compressive). Thus, the size and characteristics of TiO_2 NPs synthesized by the sol-gel method are influenced by a number of factors. The factors that impact the sol-gel process' hydrolysis and condensation processes should be managed to get TiO_2 NPs with appropriate characteristics. The pH parameters have been proven to be more essential than others.

3.3. Fourier Transform Infrared Spectroscopy (FTIR) Analysis

Figure 3 shows the FTIR spectrum for the synthesized TiO_2 NPs for acid and alkaline before and after calcination with varies in calcination temperature. FTIR spectra from Figure 3 confirmed that the surfactant there were the existence of honey's functional group as-prepared samples after three times of washing since the absorption peaks attributable to organic residuals are detected, including CH_2 and OH stretching peaks in the range of 2800 to 3000 cm^{-1} and 3000 to 3500 cm^{-1}, respectively [19-21]. The use of glucose and fructose as stabilizing and reducing agents in NPs production is gaining increasing attention these days. There have been reports that monosaccharides with a linear chain and aldehyde groups, such as glucose, are effective reducing agents, and fructose has also been discovered to be capable of contributing to the production of NPs of varied shape. In this research, honey was utilized as a reducing and stabilizing agent in the current investigation since it is a rich source of both monosaccharides. Furthermore, the most common synthesis method for TiO_2 NPs is the hydrothermal method. It assists in the synthesis of mono-dispersed and relatively homogenous NPs while ensuring effective control over their size and shape. And has the advantages of lower energy usage, improved nucleation control, and decreased emissions [22, 23]. The presence of hydrochloric acid, which are formed when honey is diluted with distilled water, may aid this decrease. Fructose has been used as a probable reducing agent in this process, while the proteins existed in honey were utilized for the stabilization of TiO_2 NPs. Another studied was carried out with and without honey during conducting this experiment to investigate how honey influenced the size of TiO_2 NPs. As shown in Table 2, it proved that honey helped as the reducing agent during the formation of TiO_2 NPs. The size of synthesized anatase obtained was 14.04 nm with the presence of honey whereas without honey the size of synthesized TiO_2 NPs is 17.77 nm. While increasing the calcination temperature the size produced with and without honey are 15.63 and 21.88 nm respectively.

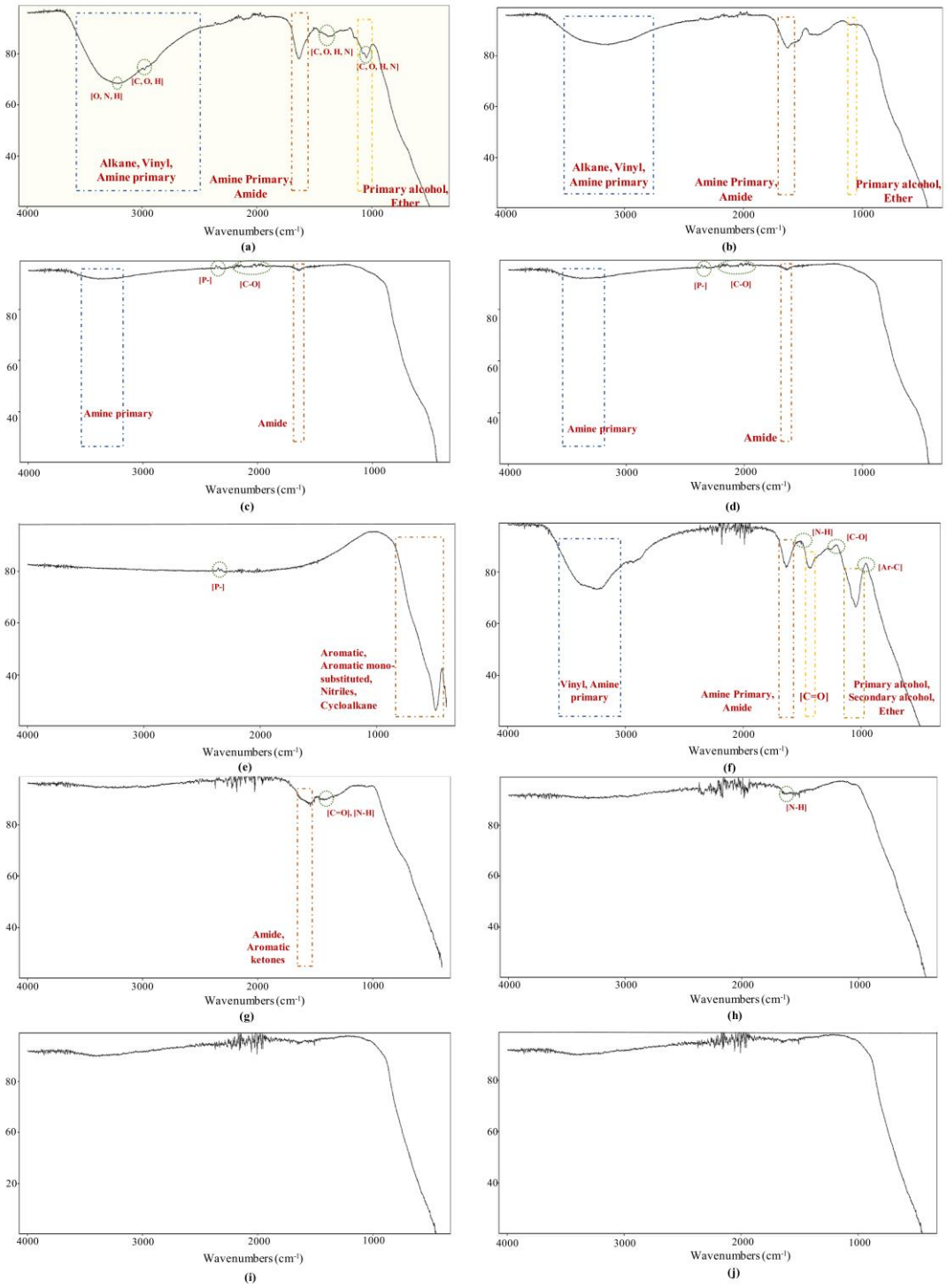

Figure 3. Presence of Honey functional group pattern in acidic and alkaline condition: (a) FTIR analysis for TiO_2 NPs before calcined in alkaline medium with honey, (b) FTIR analysis for TiO_2 NPs at 200°C in acidic medium with honey, (c) FTIR analysis for TiO_2 NPs at 400°C in acidic medium with honey, (d) FTIR analysis for TiO_2 NPs at 600°C in acidic medium with honey, (e) FTIR analysis for TiO_2 NPs at 800°C in acidic medium with honey, (f) FTIR analysis for TiO_2 NPs before calcined in alkaline medium with honey, (g) FTIR analysis for TiO_2 NPs at 200°C in alkaline medium with honey, (h) FTIR analysis for TiO_2 NPs at 400°C in alkaline medium with honey, (i) FTIR analysis for TiO_2 NPs at 600°C in alkaline medium with honey, FTIR analysis for TiO_2 NPs at 800°C in alkaline medium with honey.

4. Conclusions

In conclusion, using hydrolyzing a titanium isopropoxide alcoholic solution and then peptizing the resulting suspension at 70 °C for 18 hours, nanocrystalline TiO_2 NPs powder was successfully synthesized. Besides, the crystallite size has been decreased with existing of honey as a reducing agent. Scherrer's formula was used to determine the size of the TiO_2 NPs crystallites. The average size of TiO_2 NPs obtained is 11.84 nm when the powder is thermally treated at 400°C in acidic condition, and it is considered that a pure anatase phase were consists at this stage. The pH of the sol-gel solution used to synthesis homogeneous anatase TiO_2 particles from condensed TiO_2 gel is a significant factor in influencing the product's finished particle size and shape. When the pH of the sol rises, the grain size of the TiO_2 particles continues to rise. Because hydrogen ions interfere with the process and slow the nucleation rate, the particles develop quickly to form larger grains when the hydrogen ion concentration is high. There is enough time for the new nucleus to develop and aggregate into large TiO_2 particles. The formation of TiO_2 particles of a narrow size can be achieved by aging a very acidic titanium tetrachloride solution at severe temperatures for 12 to 18 hours. The amount of acid (pH) influences not only the size of the NPs, but also the stability of the sol. The particle size grows as the calcination temperature is raised. This research was accomplished by dispersing PLA with the synthesized TiO_2 NPs to fabricate a self-cleaning bio-based polymer characteristic.

Funding

This research was funded by CRG National Grant (R.K130000.7343.4B539) and (FRGS/1/2020/STG05/UTM/02/9).

Acknowledgement

The author are grateful for the full support from Chemical and Environmental Engineering (ChEE) Department, Malaysia-Japan International Institute of Technology (MJIIT), Universiti Teknologi Malaysia, Kuala Lumpur under funding of CRG National Grant (R.K130000.7343.4B539) and (FRGS/1/2020/STG05/UTM/02/9).

References

1. Chisenga, S.M.; Tolesa, G.N.; and Workneh, T.S. "Biodegradable Food Packaging Materials and Prospects of the Fourth Industrial Revolution for Tomato Fruit and Product Handling." *Int. J. Food Sci.* (2020): 1-18. doi: https://doi.org/10.1155/2020/8879101.
2. Han, J.W.; Ruiz-Garcia, L.; Qian, J.P.; and Yang, X.T. "Food packaging: a comprehensive review and future trends." *Compr. Rev. Food Sci. Food Saf.* 17, no. 4 (2018): 860–877, 2018. doi: https://doi.org/10.1111/1541-4337.12343.
3. Singh, N.; Hui, D.; Singh, R.; Ahuja, I.P.S.; Feo, L.; and Fraternali, F. "Recycling of plastic solid waste: a state of art review and future applications." *Compos. B. Eng.* 115 (2017): 409-422. doi: https://doi.org/10.1016/j.wasman.2016.10.006.
4. Emadian, S.M.; Onay, T.T.; and Demirel, B. "Biodegradation of bioplastics in natural environments." *Waste Management* 59 (2017): 526-536. doi: https://doi.org/10.1016/j.wasman.2016.10.006.
5. Ivanković, A.; Zeljko, K.; Talić, S.; Bevanda, A.; and Lasić, M. "biodegradable packaging in the food industry." *J. Food Qual.* 68, no. 2 (2017): 23-52. doi: 10.2376/0003-925X-.
6. Ouétchéhou, R.; Dabadé, D.D.; Vieira-Dalodé, G.G.; Sanoussi, A.F.; Fagla-Amoussou, A.B.; and et al. "Bio-based packaging used in food processing: A critical review." *Afr. J. Food Sci.* 15, no. 4 (2020): 131-144. doi: 10.5897/AJFS2020.2064.

7. Lavoine, N.; Desloges, I.; Dufresne, A.; and Bras, J. "Microfibrillated cellulose – Its barrier properties and applications in cellulosic materials: A review." *Carbohydr. Polym.* 90, no. 2 (2012): 735-764. doi: https://doi.org/10.1016/j.carbpol.2012.05.026.
8. Leminen, V.; Kainusalmi, M.; Tanninen, P.; Lindell, H.; Varis, J.; Ovaska, S.S.; and et al. "Aspects on packaging safety and biomaterials." *26th IAPRI Symposium on Packaging*, Espoo, Finland, (2013/06/10 2013).
9. Euvananont, C.; Junin, C.; Inpor, K.; Limthongkul, P.; and Thanachayanont, C. "TiO_2 optical coating layers for self-cleaning applications." *Ceram.* 34, no. 4 (2008): 1067-1071. doi: https://doi.org/10.1016/j.ceramint.2007.09.043.
10. Ragesh, P.; Anand, G.V.; Nair, S.V.; and Nair, A.S. "A review on 'self-cleaning and multifunctional materials'." *J. Mater. Chem.* 2, no. 36 (2014): 14773-14797. doi: 10.1039/c4ta02542c.
11. Oskam, G. "Metal oxide nanoparticles: synthesis, characterization and application." *J. Solgel Sci. Technol. J. Sol-Gel Sci. Techn.* 37 (2006): 161–164. doi: https://doi.org/10.1007/s10971-005-6621-2.
12. Niederberger, M. "Nonaqueous Sol–Gel Routes to Metal Oxide Nanoparticles." *Accounts of Chemical Research* 40, no. 9 (2007): 793–800. doi: https://doi.org/10.1021/ar600035e.
13. Hasnidawani, J.N.; Azlina, H.N; Norita, H.; Bonnia, N.N.; Ratim, S.; and Ali, E.S. "Synthesis of ZnO Nanostructures Using Sol-Gel Method." *Procedia Chem.* 19 (2016): 211-216. doi: https://doi.org/10.1016/j.proche.2016.03.095.
14. Cuenya, B.R. "Synthesis and catalytic properties of metal nanoparticles: Size, shape, support, composition, and oxidation state effects." *Thin Solid Films* 518, no. 12 (2010): 3127-3150. doi: https://doi.org/10.1016/j.tsf.2010.01.018.
15. Catauro, M.; Tranquillo, E.; Dal-Poggetto, G.; Pasquali, M.; Dell'Era, A.; and Vecchio-Ciprioti, S. "Influence of the Heat Treatment on the Particles Size and on the Crystalline Phase of TiO_2 Synthesized by the Sol-Gel Method." *Materials* 11, no. 12 (2018): 2364. doi: https://doi.org/10.3390/ma11122364.
16. Liu, P.; Gao, Y.; Wang, F.; Yang, J.; Yu, X.; Zhang, W.; and Yang, L. "Superhydrophobic and self-cleaning behavior of Portland cement with lotusleaf-like microstructure." *J. Clean. Prod. (Supplement C)* 156 (2017): 775-785.
17. Saad, R.S.; Abdullah, M.M.A.B.; Mahmed, N.; and Sandu, A.V. "Self-cleaning technology in fabric: A review." *IOP Conference Series: Materials Science and Engineering* 133 (2016/19/20 2016): 012028. doi: 10.1088/1757-899X/133/1/012028.
18. Ibrahim, S.A.; and Sreekantan, S. "Effect of pH on TiO_2 nanoparticles via sol gel method." International Conference on X-Rays & Related Techniques in Research & Industry, Aseania Resort Langkawi, Malaysia, (2010/06/09).
19. Jazayeri, S.D.; Ideris, A.; Zakaria, Z.; Shameli, K.; Moeini, H.; Omar, A.O. "Cytotoxicity and immunological responses following oral vaccination of nanoencapsulated avian influenza virus H5 DNA vaccine with green synthesis silver nanoparticles." *J. Control. Release.* 161(1), (2012): 116-123. doi: org/10.1016/j.jconrel.2012.04.015
20. Shameli, K.; Ahmad, M.B.; Al-Mulla, E.J.; Shabanzadeh, P.; Bagheri, S. "Antibacterial effect of silver nanoparticles on talc composites." *Res. Chem. Intermed.* 41(1), (2015), 251-263. doi:10.1007/s11164-013-1188-y
21. Jahangirian, H.; Shah Ismail, M.H.; Haron, M.H.; Rafiee-Moghaddam, R.; Shameli, K. "Synthesis and characterization of zeolite/Fe_3O_4 nanocomposite by green quick precipitation method." *Dig. J. Nanomater. Biostruct.* 8(4), (2013), 1405-1413.
22. Ahmad, M.B.; Shameli, K.; Yunus, W.M.Z.W.; Ibrahim, N.A. "Synthesis and characterization of silver/clay/chitosan bionanocomposites by UV-irradiation method." *Am. J. Appl. Sci.* 6(12), (2009), 2030.
23. Izadiyan, Z.; Shameli, K.; Hara, H.; Mohd-Taib, S. H. "Cytotoxicity assay of biosynthesis gold nanoparticles mediated by walnut (Juglans regia) green husk extract." 1151, (2018), 97-105. doi: 10.1016/j.molstruc.2017.09.039